Title
Molecular functions of the TLE tetramerization domain in Wnt target gene repression

Journal
The EMBO Journal, 33(7)

ISSN
0261-4189

Authors
Chodaparambil, Jayanth V
Pate, Kira T
Hepler, Margretta RD
et al.

Publication Date
2014-04-01

DOI
10.1002/embj.201387188

Peer reviewed

Article

TRANSPARENT PROCESS

THE EMBO JOURNAL

Molecular functions of the TLE tetramerization domain in Wnt target gene repression

Jayanth V Chodaparambil[1], Kira T Pate[2], Margretta R D Hepler[3], Becky P Tsai[2], Uma M Muthurajan[3], Karolin Luger[3], Marian L Waterman[2] & William I Weis[1,*]

Abstract

Wnt signaling activates target genes by promoting association of the co-activator β-catenin with TCF/LEF transcription factors. In the absence of β-catenin, target genes are silenced by TCF-mediated recruitment of TLE/Groucho proteins, but the molecular basis for TLE/TCF-dependent repression is unclear. We describe the unusual three-dimensional structure of the N-terminal Q domain of TLE1 that mediates tetramerization and binds to TCFs. We find that differences in repression potential of TCF/LEFs correlates with their affinities for TLE-Q, rather than direct competition between β-catenin and TLE for TCFs as part of an activation–repression switch. Structure-based mutation of the TLE tetramer interface shows that dimers cannot mediate repression, even though they bind to TCFs with the same affinity as tetramers. Furthermore, the TLE Q tetramer, not the dimer, binds to chromatin, specifically to K20 methylated histone H4 tails, suggesting that the TCF/TLE tetramer complex promotes structural transitions of chromatin to mediate repression.

Keywords chromatin; TCF/LEF; TLE/groucho; Wnt signaling
Subject Categories Signal Transduction; Structural Biology
DOI 10.1002/embj.201387188 | Received 17 October 2013 | Revised 26 January 2014 | Accepted 30 January 2014 | Published online 4 March 2014
EMBO Journal (2014) 33, 719–731

Introduction

Wnt growth factors regulate cell fate determination, patterning during embryonic development and tissue renewal in adults (Logan & Nusse, 2004; Polakis, 2007). In the Wnt/β-catenin pathway, binding of a Wnt protein to cell surface receptors inhibits destruction of the transcriptional co-activator β-catenin. The stabilized β-catenin translocates to the nucleus where it interacts with sequence-specific DNA binding TCF/LEF (T-Cell Factor/Lymphoid Enhancer Factor) proteins at Wnt-responsive elements in the promoter region of target genes. β-Catenin acts as a scaffold for the binding of chromatin remodeling complexes and general transcription activator proteins, including the histone acetyltransferase CBP/p300 (Hecht *et al*, 2000; Takemaru & Moon, 2000) and thereby activates target genes.

In the absence of Wnt and nuclear β-catenin, TCF/LEF proteins interact with transcriptional repressors of the Groucho (Gro/Grg)/Transducin-like enhancer of split (TLE) family (Arce *et al*, 2009; Cadigan & Waterman, 2012). TLE proteins regulate transcription in several signaling pathways including Ras, Notch, Wingless and Decapentaplegic (Hasson & Paroush, 2007; Turki-Judeh & Courey, 2012). TLE proteins interact with histone deacetylases (HDACs) (Chen *et al*, 1999; Arce *et al*, 2009), whose activity is important in generating transcriptionally silent chromatin. TLE proteins also bind to deacetylated histone tails (Palaparti *et al*, 1997; Flores-Saaib & Courey, 2000). Grg3, a mouse homolog of TLE1 can bind, condense and oligomerize chromatin (Sekiya & Zaret, 2007).

TLE proteins contain a conserved N-terminal glutamine-rich (Q) domain, followed by a variable central domain sub-divided into a glycine-proline rich (GP) region, the CcN and serine-proline rich (SP) regions, and a C-terminal WD40 domain that interacts with multiple transcription factors (Buscarlet & Stifani, 2007) (Fig 1A). The Q domain mediates tetramerization of TLEs (Chen *et al*, 1998) and binding to TCF/LEF proteins (Brantjes *et al*, 2001), and is essential for chromatin oligomerization (Sekiya & Zaret, 2007). In Groucho, the Q domain can also form higher oligomers, with the tetramer as the predominant species (Kuo *et al*, 2011). The GP region binds directly to HDAC1 (Chen *et al*, 1999; Billin *et al*, 2000; Brantjes *et al*, 2001). The CcN region has consensus CK2 and Cdc2 phosphorylation sites that are modified in a cell cycle-dependent manner (Nuthall *et al*, 2002). The SP region is a substrate for the Ser/Thr kinases HIPK2 and MAPK, which appear to negatively regulate transcription repression activity (Choi *et al*, 2005; Hasson *et al*, 2005), and may also interact with basic helix-loop-helix transcription factors (Fisher *et al*, 1996; Jimenez *et al*, 1997). The C-terminal WD40 domain is essential for chromatin condensation (Sekiya & Zaret, 2007) and together with SP interacts with bHLH proteins.

TCF/LEF proteins contain an N-terminal β-catenin binding sequence, followed by a Context-dependent Regulatory Domain (CRD) and a High Mobility Group (HMG) domain that binds DNA

1 Departments of Structural Biology and Molecular & Cellular Physiology, Stanford University School of Medicine, Stanford, CA, USA
2 Department of Microbiology and Molecular Genetics, University of California Irvine, Irvine, CA, USA
3 Department of Biochemistry and Molecular Biology, Colorado State University, Fort Collins, CO, USA
*Corresponding author. Tel: +1 650 725 4623; Fax: +1 650 723 8464; E-mail: bill.weis@stanford.edu

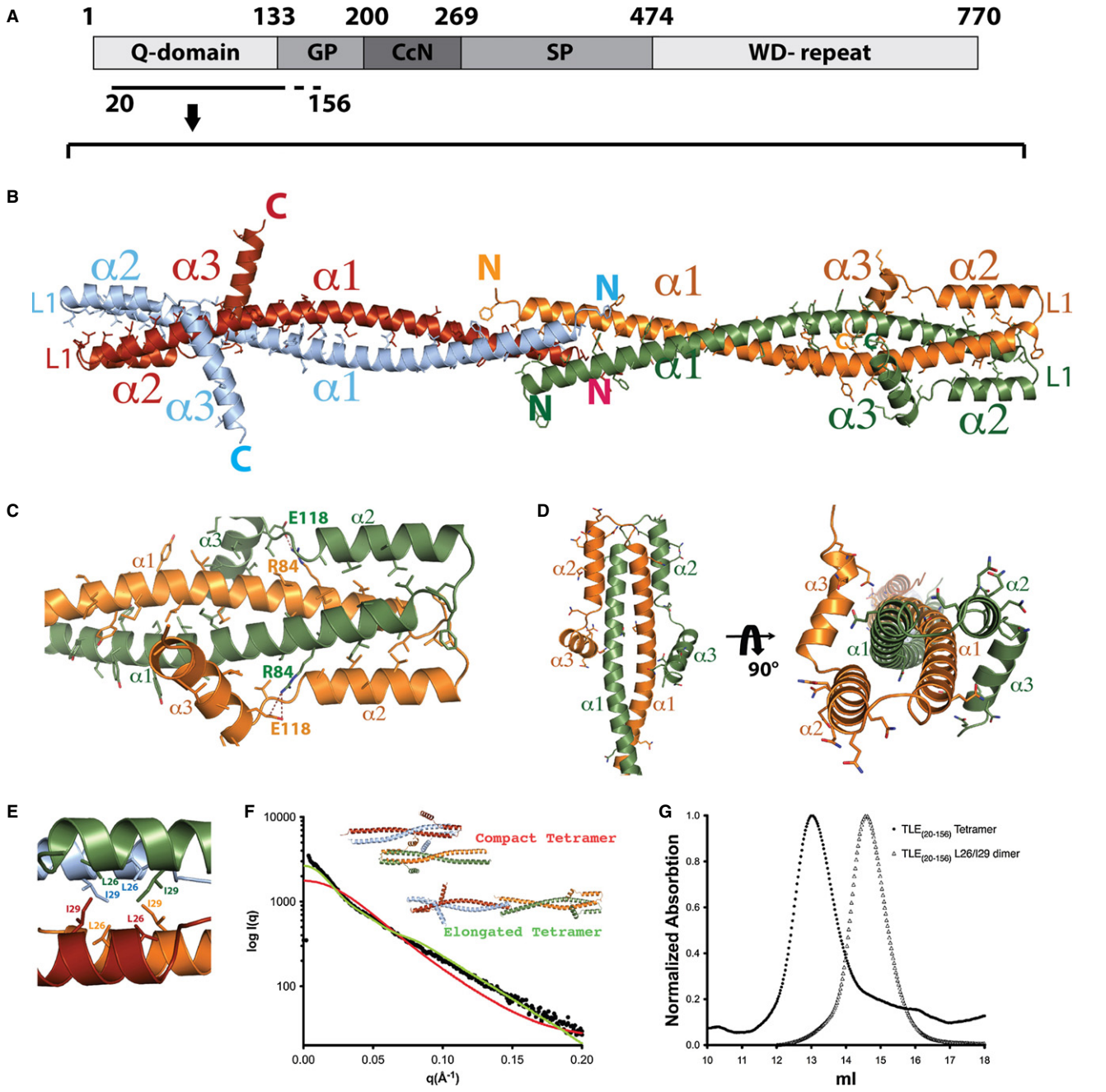

Figure 1. Structure of the TLE1 Q domain.

A The primary structure of human TLE1 showing domain boundaries.

B The structure of the TLE1 tetramerization domain comprising residues 23–136 in chains A (light blue) and B (red), and 23–133 in chains C (orange) and D (green) are shown; the remaining residues are disordered. Hydrophobic side chains are shown in stick representation, and the N- and C-termini marked.

C Hydrophobic interactions between chain C (orange) and chain D (green) involving the α2 and α3 helices. The 120° orientation between α2 and α3 is fixed by a salt bridge between E118 of one chain and R84 of its partner.

D Glutamine residues (shown in stick representation) are mostly clustered on helices α2 and α3.

E Close-up of the TLE1-Q tetramer interface.

F SAXS analysis of $TLE1_{20–156}$. The solid black line shows the experimentally determined scattering curve of $TLE1_{20–156}$ at 5 mg/ml. The R_g obtained from the Guinier plot = 70 Å, and D_{max} = 227 Å as calculated with Autognom (Semenyuk & Svergun, 1991). These values match closely the R_g = 69 Å and D_{max} = 217 Å calculated from the extended tetramer model (green line; χ^2 = 3.1) versus R_g = 35 Å and D_{max} = 162 Å for the compact tetramer (red line; χ^2 = 6.9; see Supplementary Fig S1B).

G Gel filtration of the $TLE1_{20–156}$ tetramer and L26D, I29D dimer mutant. Purified proteins were run on a Superdex S200 gel filtration column. Due to their large hydrodynamic radius (axial ratio ~10:1), the proteins run at apparent molecular weights of 173 kDa, and 53 kDa.

(Fig 2A). Although all TCF/LEFs interact with β-catenin and TLE co-repressors, gene knockout studies in vertebrate model systems have shown that TCF/LEF family members function differently from one another depending on the developmental context. Particular TCF/LEFs act predominantly as either repressors or activators in developing *Xenopus* embryos (Kim *et al*, 2000; Liu *et al*, 2005; Standley *et al*, 2006; Hikasa *et al*, 2010), mouse embryonic stem cells (Merrill *et al*, 2004; Tam *et al*, 2008; Hikasa *et al*, 2010; Yi *et al*, 2011), stem cells in embryonic skin (Nguyen *et al*, 2009), hair follicles and intestine (van de Wetering *et al*, 1997; Korinek *et al*, 1998; Roose *et al*, 1999), and in cancer cells (Tang *et al*, 2008). The most common trends are for TCF3 and TCF4 to serve as repressors, whereas TCF1 and LEF1 perform as activators. Differences in activating and repressing roles amongst TCF/LEFs map to the CRD of each protein in both genetic (Liu *et al*, 2005) and cell culture systems (Cadigan & Waterman, 2012), and deletion of the CRD eliminates repressive functions and increases transcription of target genes (Pereira *et al*, 2006; Tam *et al*, 2008; Nguyen *et al*, 2009). A study of Wnt-mediated *Xenopus* axis specification found that the repressor TCF3 is replaced by TCF1/β-catenin (Hikasa *et al*, 2010), with the switch between TCF3 and TCF1 apparently mediated by β-catenin scaffolded HIPK2 phosphorylation of residues in the TCF3 CRD. Taken together, these studies define different roles for individual TCF/LEFs in gene regulation and indicate a key role for the CRD in defining those differences.

In this work, we address the molecular basis for the different roles of TCF/LEFs in gene repression and activation in Wnt signaling. The TCF/LEF CRD is important for repression and is the most highly divergent region of TCF/LEFs. The TLE Q domain binds to the TCF/LEF CRD and is essential for transcriptional repression (Brantjes *et al*, 2001). However, it is unclear whether TLEs interact equivalently with the different TCF/LEFs, and it is not known how the Q domain can be involved simultaneously with tetramerization and TCF/LEF binding, and chromatin oligomerization. We report the three-dimensional structure of the TLE1 Q domain and an analysis of its binding interactions. We find that different affinities for the four TCF/LEF proteins correlate directly with their relative repression activities. We show that there is no competition between β-catenin and TLE1 for TCF3 binding, and we demonstrate that the Q domain tetramer binds directly to chromatin through hypoacetylated and H4K20 trimethylated histone H4 tails. These findings lead to a new model of the switch between repression and activation of Wnt target genes.

Results

The TLE Q domain is an interdigitated dimer of dimers

A construct spanning residues 20–156 of human TLE1 (Fig 1A), which includes the N-terminal Q domain and a portion of the neighboring GP region, was purified and crystallized, and the structure determined at 2.9 Å resolution (Supplementary Table S1, Supplementary Fig S1A). The asymmetric unit of the crystal contains four protomers comprising the Q domain tetramer (Supplementary Fig S1B).

Each $TLE_{20\text{-}156}$ protomer consists of a 70-amino-acid α helix (α1) followed by two short helices (α2 and α3) (Fig 1B). The long helices of two protomers associate to form an extensive parallel coiled-coil dimer, mediated by hydrophobic residues at canonical heptad *a* and *d* positions between residues 24–94 (Fig 1B and C). The dimer is further stabilized by interactions of α2 and α3 with the partner protomer (Fig 1C). Specifically, α2 (residues 102–111) packs against the C-terminal portion of the partner α1. A small non-helical stretch leads into α3 (115–134), which is bent approximately 120° relative to α2. This orientation is fixed by a salt bridge between E118 of α3 and R84 in the partner α1, as well as hydrophobic contacts between the N-terminal portion of α3 and α1 (Fig 1C). A total of 5,520 $Å^2$ of surface area is buried in the dimer interface. The glutamine residues that give rise to the name of this domain cluster on the surfaces of α2 and α3 (Fig 1D).

The Q domain tetramer forms by antiparallel association of the N-terminal portions of the dimer helices (residues 21–36) with the equivalent residues of another dimer, which produces a 212-Å elongated dimer of dimers (Fig 1B and E). The dimer-dimer interaction is mediated by hydrophobic side chains and buries 3,320 $Å^2$ of surface area. We confirmed that this unusual N-terminally interdigitated dimer of dimers is the solution structure by small-angle X-ray scattering (Fig 1F). This architecture is also consistent with previous biochemical characterization that revealed a frictional coefficient ratio $f/f_0 > 2$ for the tetramer (Kuo *et al*, 2011).

The residues that mediate the hydrophobic interactions in the tetramer interface are highly conserved amongst the TLE/Gro family (Supplementary Fig S1C), suggesting that this mode of tetramerization is an intrinsic and ancient feature. To eliminate the possibility the observed mode of association arises from removal of the first 19 TLE1 residues, we refined the structure against a 4-Å data set measured from virtually isomorphous crystals of $TLE_{1–156}$. This structure showed that the first 20 residues of the Q domain are unstructured and not involved in tetramer formation (Supplementary Fig S1A). The elongated tetramer model was tested further by selectively destabilizing the tetramer interface. Leu26 and Ile29, which interact in the interface, were both changed to aspartate. The L26D/I29D mutant eluted from a size-exclusion chromatography column at a reduced apparent molecular weight corresponding to a prolate dimer relative to the wild-type tetramer (Fig 1G), and we therefore desginate this mutant the $TLE1_{20–156}$ dimer.

The strong conservation of the Q domain tetramerization interface (Supplementary Fig S1C) suggests that heterotetramers of different family members might form to produce graded levels of repression. Heterotetramer formation could underlie the ability of AES/Grg5, a C-terminally truncated family member, to antagonize TLE repressive activity (Beagle & Johnson, 2010).

$TLE1_{20\text{-}156}$ binds to TCF3 and TCF4 but not to LEF1 and TCF1

Invertebrates possess a single TCF (e.g., *Drosophila* Pangolin) that recruits Groucho for repressor activities, or Armadillo (β-catenin) for target gene activation (van de Wetering *et al*, 1997). In contrast, vertebrates have four family members, and as described above, TCF3 and TCF4 are often associated with repressive functions, whereas TCF1 and LEF1 are more associated with target gene activation (Kim *et al*, 2000; Merrill *et al*, 2004; Liu *et al*, 2005; Tang *et al*, 2008; Nguyen *et al*, 2009). This segregation of duties is not absolute, as all family members can bind to β-catenin for activation of transcription. To compare directly their potential for transcription activation, we assessed the relative activities of TCF1, LEF1, TCF3 or TCF4 with co-expressed β-catenin in a standard TOPflash luciferase reporter assay in two different cell lines. We observed that TCF1

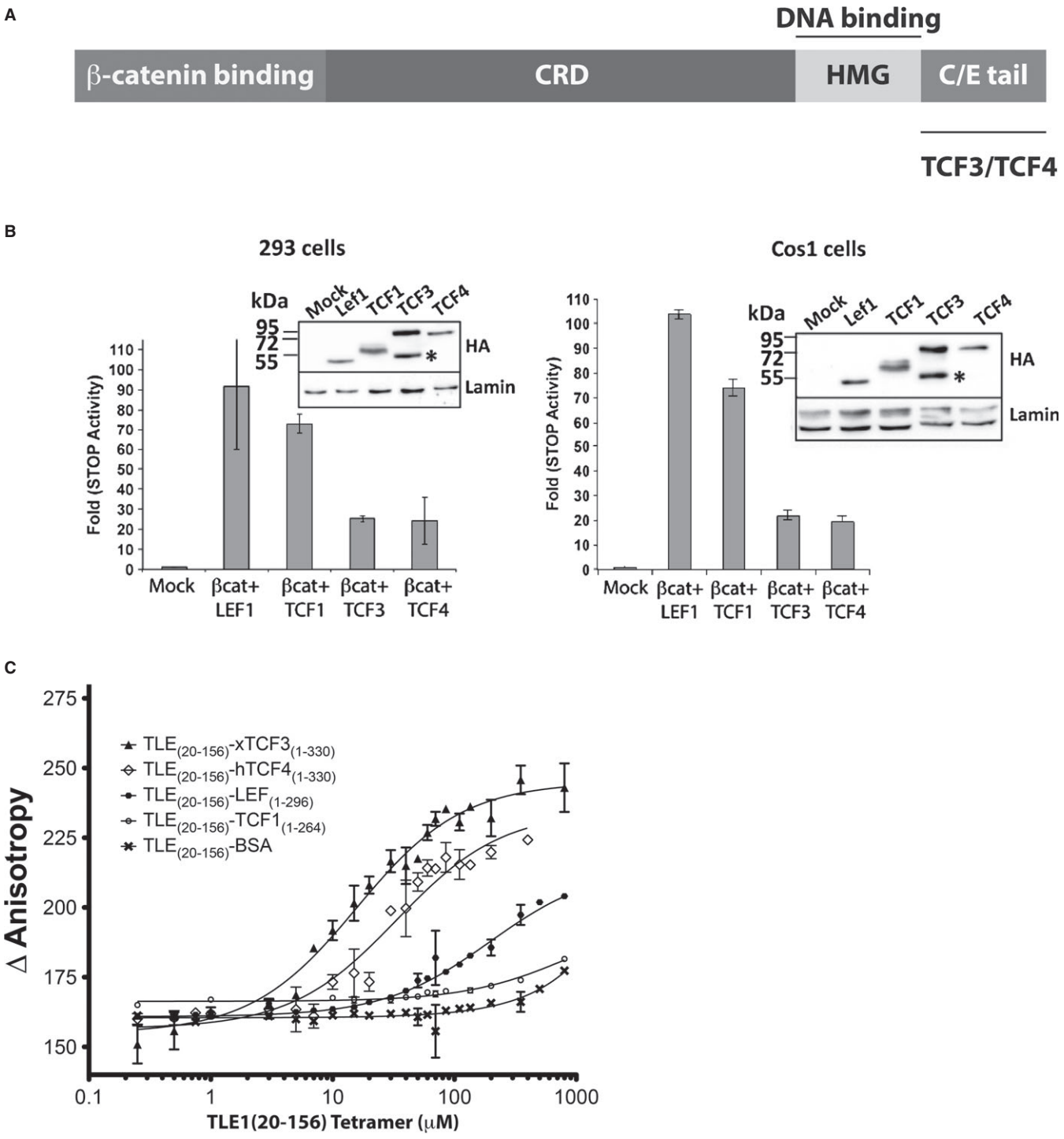

Figure 2. Reporter activity of TCF/LEF proteins correlates with affinity for TLE1.

A Primary structure of the TCF-LEF family of proteins, showing the N-terminal β-catenin binding domain, the context-dependent regulatory domain (CRD), and the HMG box that binds DNA. TCF3 and TCF4 also have extensions that arise from alternative splicing. Residue numbers for domain boundaries are shown for the XTCF3 protein used in this study. The equivalent sequence numbers of other family members can be found in Supplementary Fig S2.

B Luciferase reporter assay in HEK293 cells (left) and Cos1 cells (right) shows differential abilities of transfected HA-tagged TCF/LEFs to activate the Wnt reporter SuperTOPFlash when co-transfected with β-catenin. The graphs for each cell line are representative of three replicates. The Western blots (anti-HA) shown in the insets reveal the relative expression levels of the transfected TCF/LEF constructs and show that the activity differences are not related to protein levels. The band marked * is a breakdown product of TCF3. Error bars represent the standard deviation of triplicate measurements.

C Fluorescence anisotropy analysis of $TLE1_{20–156}$ binding to different TCF/LEFs. Increasing amounts of TCF/LEF ligands were titrated against labeled $TLE1_{20–156}$. The change in anisotropy was measured and plotted as a function of concentration. Error bars represent standard deviation of triplicate measurements.

and LEF1 directed the highest reporter activity, much more than TCF3 and TCF4, even though they are equivalently expressed (Fig 2B). These results extend similar findings in HEK293 cells (Brantjes *et al*, 2001), and indicate that there are inherent differences in the ability of TCF/LEFs to mediate transcription activation.

β-catenin binds with similar high affinities (~20 nM K_D) to the β-catenin binding domain of each TCF/LEF (Knapp *et al*, 2001; Sun & Weis, 2011), so we hypothesized that the differences in TOPflash activation reflect differences in their binding affinity for endogenous TLE repressor proteins. We used fluorescence anisotropy of labeled $TLE1_{20–156}$ to measure its affinity for purified mLEF1, hTCF1, xTCF3 and hTCF4 constructs lacking their HMG domains, a separate region that does not contribute to TLE interactions (Arce *et al*, 2009). $TLE1_{20-156}$ binds to TCF3 and TCF4 with K_Ds of 16 μm and 34 μM respectively, whereas it binds LEF1 and TCF1 with K_Ds of 195 μM and 1 mM (Fig 2C, Table 1). Although interactions of other regions in TCFs undoubtedly have a role in determining activating versus repressive activity, these results demonstrate that TCF3 and TCF4 can form repressive complexes with TLE1 more readily than can LEF1 and TCF1.

β-catenin and $TLE1_{20–156}$ bind to distinct regions of TCF3 and do not compete for TCF3

We used TCF3 deletion constructs to define the region that binds to the $TLE1_{20–156}$ tetramer (Table 1). Our data indicate that the principal interaction region of TCF3 spans residues 65–200, with weaker contributions from residues between 200 and 330. This is consistent with earlier deletion studies (Daniels & Weis, 2005; Arce *et al*, 2009) as well as studies in *Xenopus* that highlighted this region in TCF/LEFs as the key difference for repression and activation roles (Liu *et al*, 2005; Nguyen *et al*, 2009). Shorter constructs designed to define the binding site more precisely proved too unstable to purify. Nonetheless, the data show the $TLE1_{20–156}$ interaction involves more than the region equivalent to residues 216–256 of LEF1 described previously (Daniels & Weis, 2005; Arce *et al*, 2009).

Table 1. Binding affinities of TCF/LEFs to the $TLE1_{20–156}$ tetramer and L26D/I29D dimer.

	Tetramer	Dimer
Complex	**K_D ± s.d. (μM)**	**K_D ± s.d. (μM)**
Binding to different TCF/LEF family members		
$TLE1_{(20–156)}$: $LEF1_{(1–296)}$	195 ± 7	N.D.
$TLE1_{(20–156)}$: $TCF1_{(1–264)}$	1023 ± 465	N.D.
$TLE1_{(20–156)}$: $TCF3_{(1–330)}$	16 ± 2	25 ± 5
$TLE1_{(20–156)}$: $TCF4_{(1–300)}$	34 ± 7	40 ± 8
Mapping the TCF3 binding site		
$TLE1_{(20–156)}$: $TCF3_{(1–65)}$	N.D.	
$TLE1_{(20–156)}$: $TCF3_{(1–131)}$	33 ± 7	
$TLE1_{(20–156)}$: $TCF3_{(131–330)}$	9 ± 1	
$TLE1_{(20–156)}$: $TCF3_{(200–330)}$	126 ± 35	
$TLE1_{(20–156)}$: $TCF3_{(Δ131–162)}$	42 ± 6	
Control binding to BSA		
$TLE1_{(20–156)}$: Bovine Serum Albumin	N.D.	N.D.

Standard deviation corresponds to $n = 3$, N.D.: not detected.

Earlier studies indicated that β-catenin could compete directly with TLE1 Q domain for binding to LEF1, suggesting that the switch from repression to activation upon Wnt signaling is due to direct competition for TCF/LEF as the levels of nuclear β-catenin rise (Daniels & Weis, 2005). Our data confirm that the β-catenin binding domain of TCF3 (residues 1–65) does not contribute to TLE1 binding (Table 1). We also find that LEF1 binds very weakly to TLE1. As the previous study used shorter TLE protein constructs that were poorly soluble and sensitive to pH (Daniels & Weis, 2005), we retested the competition model using our well-behaved $TLE1_{20–156}$ fragment with repressive TCF3. Since the binding affinity is only 16 μM, we purified the β-catenin-$TCF3_{1–330}$ complex (K_Ds for β-catenin binding to the highly homologous LEF1 1–131 and TCF4 1–53 are 10 and 20 nM, respectively (Daniels & Weis, 2005; Fasolini *et al*, 2003; Sun & Weis, 2011)), and titrated increasing concentrations of this complex into labeled $TLE1_{20–156}$. The affinity of $TLE1_{20–156}$ for the β-catenin–TCF3 complex was 14 ± 1 μM, essentially the same as the $TLE1_{20–156}$-TCF3 interaction (Fig 3A). These data demonstrate that there is no competition between β-catenin and $TLE1_{20–156}$ and, consistent with the domain mapping data (Table 1), that the binding regions for β-catenin and $TLE1_{20–156}$ on TCF3 are independent of one another.

The finding that TCF3–TLE1 complexes are exchanged for TCF1–β-catenin complexes at a Wnt target gene promoter during *Xenopus* development, and that HIPK2-mediated phosphorylation of sites within amino acids 131–160 of TCF3 facilitates this switch, suggested that TLE binding might require residues in this region (Hikasa *et al*, 2010). The sequence equivalent to TCF3 131–160 is similar in TCF4, but differs significantly from the equivalent region in TCF1 and LEF1 (Supplementary Fig S2). To test the role of this region in TLE1 binding, we made a TCF3 construct lacking residues 130–162. $TLE1_{20–156}$ bound to this deletion mutant with a K_D of 42 μM, only slightly weaker than constructs containing this region. Thus, the non-phosphorylated 131–160 sequence contributes only modestly to TLE binding, and suggests that phosphorylation might non-specifically prevent binding by electrostatic repulsion, and/or promote binding of another factor that removes TLE from TCF.

Tetramerization is essential for repression *in vivo*

The $TLE1_{20–156}$ L26D/I29D mutant selectively disrupts the tetramer without destroying the dimeric building block (Fig 1G), so we tested whether the dimer can still interact with TCF/LEF proteins. $TLE1_{20–156}$ mutant dimer binds to TCF3 and TCF4 with the same affinity as the wild-type tetramer (Fig 3B). This demonstrates that the dimer confers full binding to TCF3 and TCF4, and it suggests that the stoichiometry of TLE-TCF interaction is unlikely to be 4:1 TLE:TCF as reported (Daniels & Weis, 2005).

We next tested whether the TLE1 dimer can function as a co-repressor for transcription using a standard TOPflash assay. Co-expression of TCF3 and β-catenin caused modest repression of TOPflash even in the absence of Wnt activation (Fig 3C), presumably because TCF3 was preferentially working through endogenous TLE proteins. When wild-type TLE1 was co-expressed, strong repression was observed (Fig 3C and D), whereas co-expression of the TLE1 dimer mutant showed little repression (Fig 3D). These data indicate that tetramerization of the TLE1 Q domain has additional critical functions in repression beyond binding to TCF proteins.

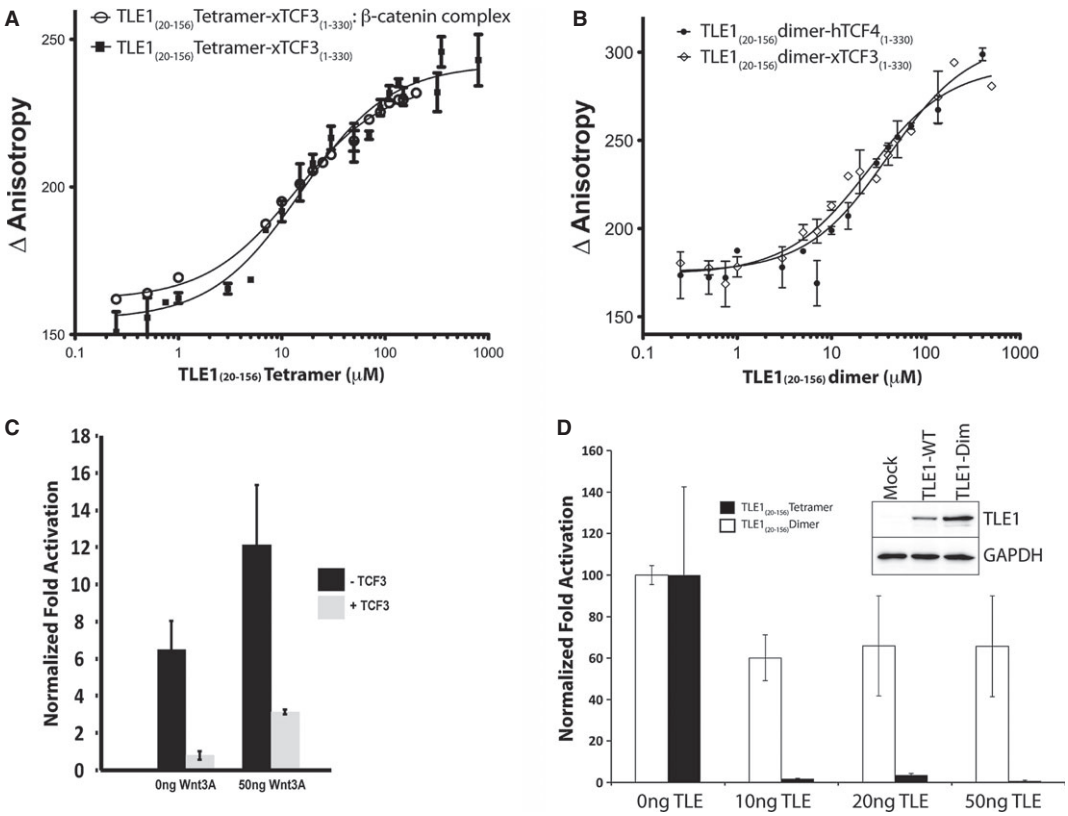

Figure 3. $TLE1_{20–156}$ tetramer and dimer can bind TCF3 and TCF4 *in vitro*, but only the tetramer represses transcription *in vivo*.

A Binding of $TLE1_{20–156}$ tetramer to the $TCF3_{(1–330)}$: β-catenin complex or $TCF3_{1–330}$ measured by fluorescence anisotropy. Error bars represent standard deviation of $n = 3$.

B Binding of $TLE1_{20–156}$ dimer mutant to and $TCF3_{1–330}$ and $TCF4_{1–330}$. Error bars represent standard deviation of $n = 3$.

C Overexpression of TCF3 leads to significant repression of reporter activity in HEK293T cells. Cells were treated with 50 ng of purified Wnt3a 24 h after co-transfection with or without TCF3. Error bars represent standard deviation of $n = 3$.

D TLE tetramer but not the dimer can repress reporter activity in HEK293T cells. Cells were treated with 100 ng of purified Wnt3a 24 h after co-transfection with β-catenin, TCF3 and indicated amounts of DNA constructs encoding either TLE1 dimer or TLE1 tetramer. Error bars represent standard deviation of $n = 3$. Inset Western blot shows levels of transfected TLE1 tetramer or dimer. Immunofluorescence demonstrating nuclear localization of transfectred TLE1 constructs is shown in Supplementary Fig S3.

$TLE1_{20–156}$ binds directly to chromatin

Grg3, a mouse homolog of TLE1, binds to, condenses and oligomerizes chromatin into a higher-order structure. The compaction/condensation activity (short-range or *cis* interactions between nucleosomes) depends on the C-terminal WD domain, whereas the Q domain is needed for oligomerization (long-range or *trans* interactions) that create higher-order, transcriptionally silent chromatin structure. However, the molecular basis of Q domain involvement in this process is not clear (Sekiya & Zaret, 2007).

As Q domain tetramerization is important for transcription repression *in vivo* (Fig 3D) but not for TCF/LEF binding, we tested binding of wild-type $TLE1_{20–156}$ tetramer or the $TLE1_{20-156}$ dimer to tri-nucleosomes using a FRET-based assay. Trinucleosome arrays provide a minimal system to study nucleosome interactions in a chromatin context (Winkler *et al*, 2011). The tetramer bound to tri-nucleosomes with a K_D of 423 nM, whereas the dimer did not approach saturation, preventing accurate affinity determination and indicating a weak interaction with $K_D > 2$ μM (Fig 4A).

The surface electrostatic potential of the TLE1 tetramer features a positively charged region at the N-terminal tetramerization region separating strongly negatively charged surfaces that run along the parallel dimer (Fig 4B). We hypothesized that the acidic surface of the Q domain binds to highly basic histone tails. The binding of synthetic biotinylated histone tails to the $TLE1_{20–156}$ tetramer and dimer mutant was analyzed using native gel shifts to obtain relative binding affinities. The $TLE1_{20–156}$ tetramer bound to unmodified H4 and H4 trimethylated at lysine 20 (H4K20Me3; associated with heterochromatin) tails with apparent K_Ds of 42 and 13 μM, respectively (Fig 4C). The dimer also bound to these tails (Fig 4D). Binding to H2A, H2B and H3 was significantly weaker for both the tetramer and dimer (Fig 4C and D). The increase in affinity of H4K20Me3 versus unmodified H4 for the tetramer may indicate that regions closer to the C-terminal portion of the tail participate in the interaction with the TLE1 Q domain.

The H4 tail plays an important role in chromatin condensation and oligomerization (Dorigo *et al*, 2003). We therefore tested whether a euchromatic form of hyper-acetylated H4 tail affected

$TLE1_{20–156}$ binding. Both the wild-type and dimer mutant $TLE1_{20–156}$ bound only weakly, probably non-specifically, to hyper-acetylated H4 tails (82 and 257 μM for tetramer and dimer, respectively; Fig 4C and D), consistent with the role of TLE1 as a repressor. Even though the unmodified H3 tail binds more weakly or non-specifically to $TLE_{20–156}$, we also tested whether the H3K27Me and the H3K9Me modified tails, which are associated with transcriptionally silent chromatin, bind to the $TLE_{20–156}$. H3K27Me and H3K9Me tails bound to $TLE_{20–156}$ tetramer with an affinity of ~424 μM and ~185 μM respectively, and the $TLE_{20–156}$ dimer bound to them with affinities of ~1.5 mM and ~420 μM respectively, indicating that the tetramerization domain preferentially interacts with K20 methylated H4 tails.

Discussion

The TLE Q domain is critical for transcriptional repression generally and for Wnt target genes in particular (Song *et al*, 2004; Sekiya & Zaret, 2007). The structural and biochemical data presented here provide several key insights into TLE/Gro-mediated repression, including its role in the switch from repression to Wnt-dependent activation.

Earlier studies hypothesized that the switch from repression to activation was mediated by β-catenin directly competing and displacing TLE1 from target-bound TCF/LEFs upon Wnt stimulation (Daniels & Weis, 2005). Our data are inconsistent with this model, as the presence of β-catenin does not alter the affinity of the TCF3-$TLE1_{20–156}$ interaction. Nonetheless, chromatin immunoprecipitation data indicate that β-catenin and TLE1 are present on chromatin targets in a mutually exclusive manner during Wnt pathway activation (Sierra *et al*, 2006). Thus, there must be a mechanism for exchange of TLE and β-catenin other than simple competitive binding (Sierra *et al*, 2006).

Since β-catenin binds to TCF/LEF proteins with very similar affinity (Knapp *et al*, 2001; Sun & Weis, 2011), the differences in the affinity of TLE for TCF/LEF (Table 1) go much further to explain the tendencies of different TCF/LEF proteins to repress or activate genes. Our data show that under identical conditions, TCF/LEFs display sharply different levels of Wnt-stimulated activation, a range of activities that directly correlates with their affinities for TLE1. Although the affinities of the Q domain for even the repressive TCFs are relatively weak, these differences may be significant in the context of chromatin, since other regions of TLEs interact with the H3 tails (Flores-Saaib & Courey, 2000; Sekiya & Zaret, 2007), and the TCFs are bound to DNA. Thus, multiple contacts involving TLE, TCF and chromatin contribute to the overall stability of the repressive complex, and other factors such as post-translational modification also have a role. Note that the TLE-TCF binding experiments reported here were done with TCF constructs lacking the DNA-binding HMG domain. Binding of the TCF to DNA could create additional interacting surfaces that stabilize the TLE-TCF-chromatin interactions.

Post-translational modifications of both TLE1 and TCFs appear to have critical roles in removing TLE proteins from TCFs as part of the switch from repression to activation. Recently, the ubiquitin E3 ligase X-linked inhibitor of apoptosis (XIAP), which is a positive regulator of Wnt signaling, was shown to ubiquitylate TLE proteins and thereby decrease binding to TCF/LEF (Hanson *et al*, 2012). Furthermore, the Ser/Thr kinase HIPK2 can up-regulate Wnt signaling through phosphorylation of several targets, including TLE1 and TCF/LEF (Choi *et al*, 2005; Lee *et al*, 2009; Hikasa *et al*, 2010). Phosphorylation of Groucho by HIPK2 and possibly MAPK weakens its co-repressor activity by promoting its dissociation from the co-repressor complex (Choi *et al*, 2005). In vertebrates, TCF3, TCF4 and LEF1 are phosphorylated at multiple sites by HIPK2 upon Wnt stimulation, and phosphorylation of TCF3 leads to its loss from promoter regions and replacement by TCF1 (Hikasa *et al*, 2010).

The mechanism through which HIPK2 phosphorylation mediates a switch in TCF-repressor for TCF-activator complexes is unclear, but it is important to note that three HIPK2 phosphorylation sites are found between residues 131 and 200 of TCF3 and TCF4, the same region that is required for interaction with TLE1 (Supplementary Fig S2). Two of the three sites are present in LEF1, but all are absent in TCF1 (Hikasa & Sokol, 2011). Since HIPK2 phosphorylation decreases TCF binding to promoter regions (Hikasa & Sokol, 2011), we suggest that HIPK2 phosphorylation of both TCF3 and TLE1 disrupts their interaction with each other and with DNA and thereby promotes their loss from promoter regions. Replacement of TCF3 by TCF1, which does not bind to TLE and does not have HIPK2 sites, would ensure that only activating complexes are formed at a Wnt response element. Note that replacement of one TCF for another is unlikely to be a general mechanism in Wnt target gene activation, as some organisms possess only a single TCF. Nonetheless, post-translational modifications appear to be common: for example, in *Drosophila* the increase in nuclear β-catenin levels upon Wnt activation affects the displacement of HDAC1 from the groucho-dTCF complex (Billin *et al*, 2000). Furthermore, the groucho-TCF repression complex is weakened by DHIPK2 phosphorylation of both groucho and TCF (Choi *et al*, 2005), followed by β-catenin binding to TCF and chromatin opening for transcription activation.

TLE interactions with chromatin

Gro/TLE proteins promote formation of transcriptionally silent chromatin through direct interactions with histones as well by scaffolding enzymes that modify histones. Repression by Gro/TLE proteins requires an intact Q domain (Song *et al*, 2004), and studies of Grg3 have shown that the Q domain is needed for chromatin oligomerization (long range *trans* interactions), whereas the C-terminal WD domain is essential for condensation (short range *cis*-interactions) (Sekiya & Zaret, 2007).

We found that the TLE1 Q domain tetramer can bind specifically to chromatin (Fig 4), at least in part through interaction with H4 tails. Although we have not been able to determine the stoichiometry of this interaction, the fact that the Q domain dimer mutant also binds to the H4 tails suggests that the tetramer can bind at least two H4 tails. Given the elongated structure of the Q domain, it is likely that one role of the tetramer is to crosslink non-contiguous regions of chromatin by binding to H4 tails, thereby contributing to chromatin oligomerization. Trinucleosomes bind to the $TLE1_{20–156}$ tetramer much more strongly than to the dimer mutant (Fig 4A). This difference may simply be due to the multivalent nature of this interaction, but we cannot rule out additional interactions unique to the Q domain tetramer with the nucleosome core. For example, the Q domain tetramer has a positively charged surface (Fig 4B) that would be disrupted in the dimer mutant. We speculate that once TLE1 tethers itself to the nucleosome via histone tails, this positively

charged surface forms additional interactions with acidic patches on the nucleosome that are formed by the dimerization of H2A and H2B (Supplementary Fig S5). This surface is known to bind other proteins that have a direct role in condensation and oligomerization of chromatin (Dorigo *et al*, 2003; Barbera *et al*, 2006; Chodaparambil *et al*, 2007; Zhou *et al*, 2007).

The TLE1 Q domain can bind to H4K20-trimethylated tails, a hallmark of heterochromatin, but not the H4-hyperacetylated tail, a characteristic of euchromatin (Fig 4C). This correlates with the observation that chromatin-bound Grg4 assists in recruitment of polycomb group proteins, which include methyl transferases, thereby epigenetically driving chromatin condensation and gene silencing (Patel *et al*, 2012).

Our data are consistent with the following general model of TLE1 in Wnt target gene repression in vertebrates (Fig 5). In the absence of Wnt signaling, TCF3 or TCF4 bound to a Wnt response element in the promoter region of a target gene recruits TLE1 by binding to the Q domain. TLE1 promotes formation of silenced chromatin through interactions with histone tails and the nucleosomal surface. TLE-mediated recruitment of HDACs and histone methyltransferases leads to local deacetylation and methylation of histone tails, enabling TLE to form silenced chromatin structures through interactions with histone tails and the nucleosomal surface (Fig 5, left). Wnt activation results in nuclear import of β-catenin, and post-translational modifications of TLE and TCF, such as phosphorylation by HIPK2 (imported with β-catenin; (Hikasa *et al*, 2010)) and ubiquitination by XIAP (Hanson *et al*, 2012), remove the repressive TCF–TLE complex from the promoter (Fig 5, middle). Clearance of repressive complexes allows activating complexes of TCFs, β-catenin, and associated chromatin remodeling factors including histone acetyl transferases CBP/p300 to bind at these sites, generating an open chromatin state that can actively participate in transcription (Fig 5, right). The Pygopus–Legless/Bcl9 complex, which has important roles in Wnt/β-catenin transciption (Jessen *et al*, 2008; Cadigan & Waterman, 2012) and binds to β-catenin and to methylated K4 H3 tails that mark active chromatin (Berger, 2007; Fiedler *et al*, 2008; Gu *et al*, 2009; Suganuma & Workman, 2011), would reinforce the switch to a transcriptionally active state, as might other modulators of transcription, such as the ring-finger protein RNF-14 that binds to TCFs and appears to stabilize β-catenin occupancy (Wu *et al*, 2013). Taken together, our data link the specific interactions between TLEs and TCFs to the more global actions of TLE-induced chromatin oligomerization and compaction. Our findings highlight how sharp differences in TLE1 affinity for TCF/LEF family members form the basis for a switch-in/switch-out of activating versus repressing complexes and stable changes in transcription and chromatin states.

Materials and Methods

Protein constructs, expression and purification

$TLE1_{1–156}$ and $TLE1_{20–156}$ were sub-cloned into a TEV protease-cleavable, N-terminal 6× histidine-tagged pPROEX vector from a full-length human TLE1 cDNA. The protein was expressed in *E. coli* BL21DE3 cells grown in LB broth at 37°C to an optical density of 0.6 and induced with 1 mM IPTG. After induction, the cells were grown for 16 h at 37°C. Expressed TLE1 proteins were purified from inclusion bodies via centrifugation at 9,000 × *g*, resuspension in phosphate buffered saline (PBS; pH 7.4) and lysis with an Emulsiflex cell disruptor. The lysate was centrifuged at 27,000 × *g* for 20 min, and the pellet washed with PBS by re-suspension and centrifugation. Inclusion bodies were solubilized in 6 M guanidine hydrochloride, 25 mM Tris pH 8.5 and 500 mM NaCl (GTN buffer), and the solution clarified by centrifugation at 27,000 × *g* for 10 min. The supernatant containing TLE1 was loaded onto a Talon resin column equilibrated in GTN buffer and incubated 3 h on a rotary shaker at 4°C. The column was washed with GTN buffer containing 5 mM imidazole and eluted with the GTN buffer containing 250 mM imidazole. To refold the protein, 1M L-arginine hydrochloride, 20% glycerol and β-mercaptoethanol was added to the eluate, then dialyzed against a buffer containing 25 mM Tris pH 8.5, 500 mM L-arginine hydrochloride, 500 mM NaCl, 20% glycerol, 5 mM EDTA, 5 mM β-mercaptoethanol for 16 h at 4°C. After the first dialysis, 1 mg of TEV protease was added to cleave the His_6-tag while further dialyzing it against 25 mM Tris pH 8.5, 150 mM NaCl, 2% glycerol, 5 mM EDTA and 5 mM β-mercaptoethanol and further purified on a Superdex S200 gel filtration column.

TCF/LEF proteins lacking their DNA-binding HMG domains, including *Xenopus* TCF3 amino acids 1-330, human TCF4 1-300, human TCF1 1-171, and mouse LEF1 1-296 were expressed in *E. coli* BL21DE3 RIL cells. These TCF/LEF proteins and full-length β-catenin were purified as described (Sun & Weis, 2011).

Crystallographic procedures

$TLE_{1–156}$ crystals grown in 100 mM Tris pH 8.5, 150 mM sodium citrate, 10% PEG400 were crushed and cross-seeded into 200 mM sodium thiocyanate, 15% PEG3350 to yield plates with approximate dimensions 30 × 10 × 75 μm^3. The crystals were harvested in the mother liquor containing 25% PEG400 as a cryoprotectant. Diffraction data were measured in 1° rotation frames for 5 s per frame on a MAR-CCD detector, using a 10-micron beam (Supplementary Table S1). The data were integrated with Mosflm and scaled using CCP4-Scala (Winn *et al*, 2011). Data extending to 4.0 Å were obtained from these crystals, but were strongly anisotropic and extended only to 7 Å along the *a*-axis. Data collection statistics are provided in Supplementary Table S1.

To improve the crystals, a construct lacking residues 1–19, $TLE1_{20-156}$, was produced. $TLE1_{20-156}$ was concentrated to 15 mg/ml, and crystals grown at 25°C by hanging drop vapor diffusion against a reservoir of 0.1 M HEPES pH 7.0 or 7.5, 15% Tacsimate pH 7.0, 10% PEG 3350, 10% 2-methyl, 2,4-pentanediol (MPD) and 100 mM RbCl. Crystals appeared after 10 days and were 150 × 50 × 10 μm^3 leaf-shaped plates. For SIRAS phasing, a mother liquor solution containing 10 mM mercury nitrophenol was added to crystal-containing drops to a final concentration of 1.5 mM and soaked for 4 days. Native and derivative crystals were washed in the mother liquor with 20% glycerol as cryoprotectant and flash frozen in liquid nitrogen. Data were measured using a 10-micron beam in 0.5° rotation frames for 2 s per frame on a Pilatus 6M pixel array detector. Anomalous scattering data from the Hg derivative were collected using inverse beam geometry. The data were integrated with XDS (Kabsch, 2010) and scaled using CCP4-Scala (Winn *et al*, 2011). Data extending to 2.9 Å were obtained for both native and

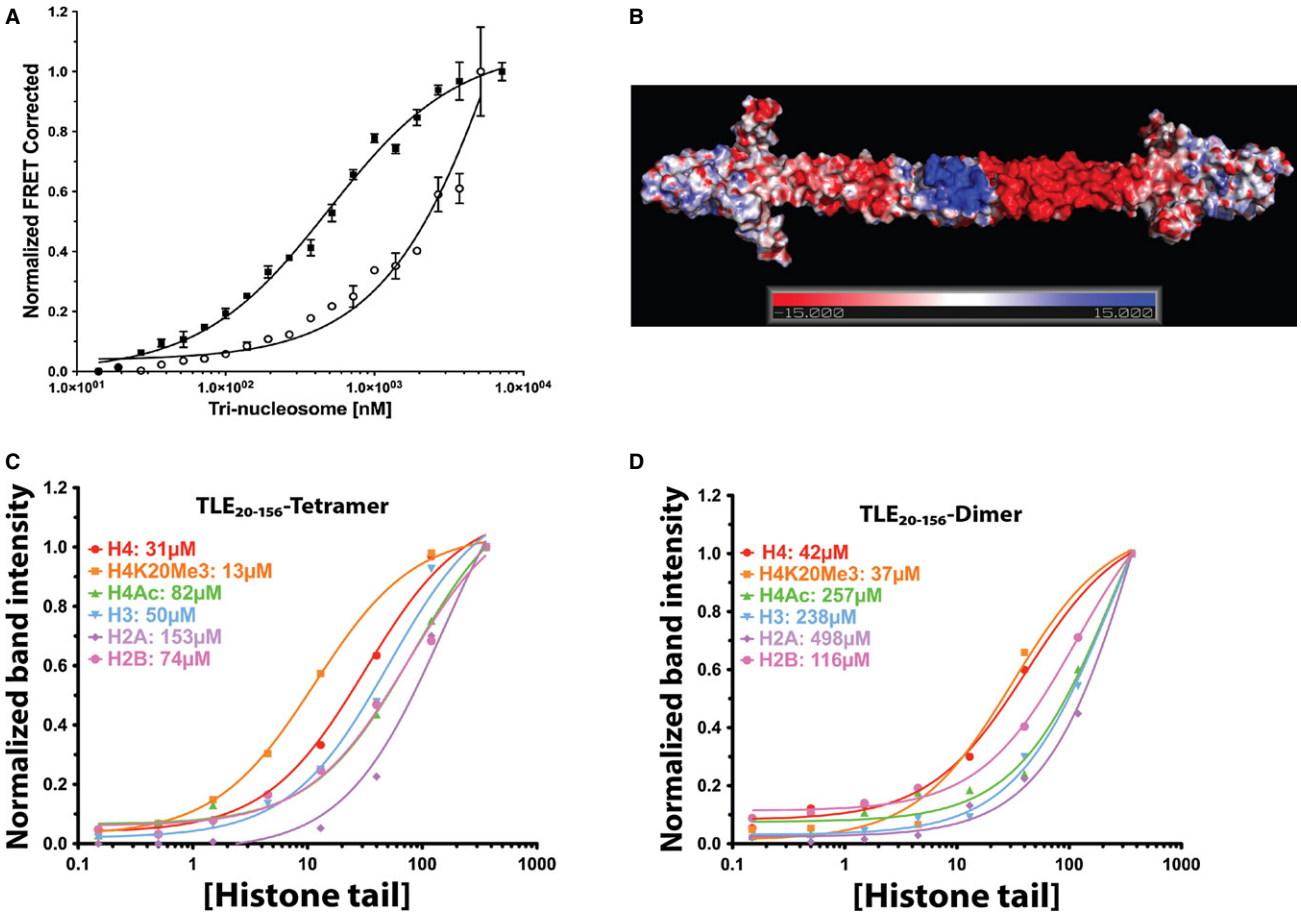

Figure 4. $TLE1_{20–156}$ tetramer but not the dimer binds to chromatin.

A Binding between fluorescently labeled tri-nucleosomes and $TLE1_{20–156}$ tetramer (square), or $TLE_{20–156}$ dimer (open circles). The FRET signal is plotted as a function of Tri-nucleosome concentration. Error bars represent standard deviation of triplicate measurements.

B Electrostatic surface representation of the $TLE1_{20–156}$ tetramerization domain, contoured between −15 k_BT and +15 k_BT. The regions shown in blue are positively charged and the regions in red are negatively charged.

C, D $TLE1_{20–156}$ interaction with histone tails. $TLE1_{20–156}$ tetramer (C) or dimer (D) were incubated with the increasing concentration of biotinylated histone tails for 16 h at 4°C. The complexes were run on a native gel and probed with NeutrAvidin-800. The highly basic histone tails enter the gel only if bound to the TLE fragment. Gel bands were quantified using ImageJ and used to determine apparent K_D values. The H4-hyperacetylated tails are labeled as H4Ac and the H4K20-trimethylated tails are represented as H4K20Me3.

derivative crystals, but the data were strongly anisotropic and extended only to 3.8 Å along the *a*-axis. Data collection statistics are provided in Supplementary Table S1.

The Hg derivative showed a significant anomalous scattering signal to 4.5 Å. Using Autosharp (Schiltz & Bricogne, 2007), six mercury sites were found and used for Single wavelength Isomorphous Replacement with Anomalous Scattering phasing. Solvent flattened maps showed long helical density. A partial poly-alanine chain was built and subjected to one round of refinement, which allowed addition of a few side chains in the core of the structure. After another round of refinement, the side chains were more pronounced. The auto-build function in Buccaneer (Cowtan, 2006) was used to complete a majority of the structure, which after refinement reduced R_{free} from 46% to 38%. NCS restraints were unhelpful and not applied during refinement. Experimental phase restraints (MLHL target) were imposed for the first few rounds of refinement in order to minimize model bias. Strict secondary structure restraints were also used throughout the refinement. The initial rounds of refinement used the MLHL target in Phenix with the SIRAS phases. After the majority of the structure was built, isotropic temperature factors and TLS-parameters were refined. Structure validation was done with Procheck (Laskowski *et al*, 1993). All structure figures were prepared with PyMol and the electrostatic potential was calculated using APBS (Baker *et al*, 2001). The final refinement statistics are summarized in Supplementary Table S1.

Initial phases for the $TLE_{1–156}$ structure were obtained by molecular replacement with AutoMR (Adams *et al*, 2010), using the crystal structure of the $TLE_{20–156}$, and refined with Phenix (Adams *et al*, 2010). The geometry of the final model was validated using MolProbity (Chen *et al*, 2010). Final refinement statistics are summarized in Supplementary Table S1.

Coordinates and structure factors for $TLE_{1–156}$ and $TLE1_{20–156}$ have been deposited in the Protein Data Bank with codes 4OM2 and 4OM3, respectively.

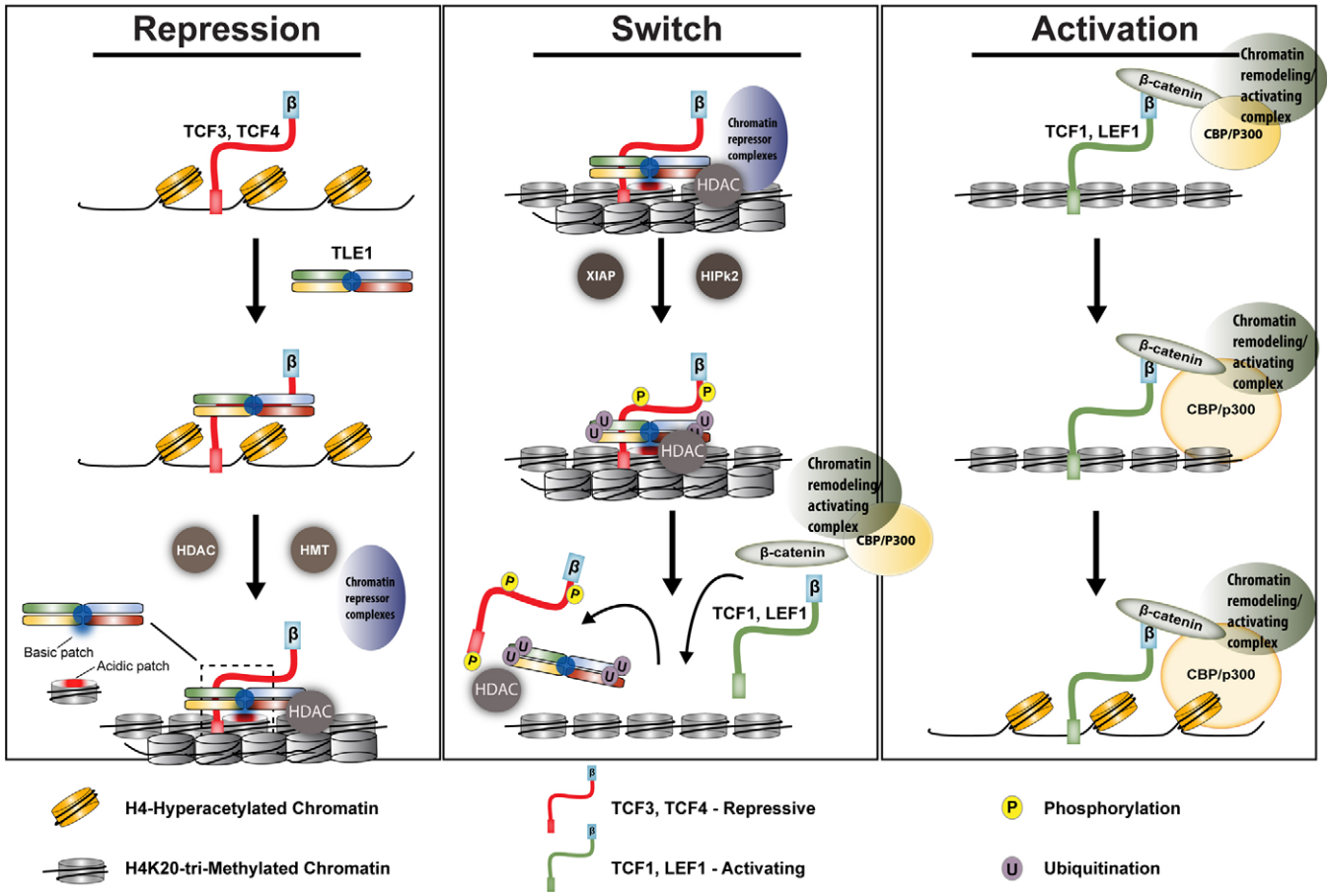

Figure 5. Model for TLE1 in Wnt signaling.
See text for detailed description.

Small angle X-ray scattering

Small angle X-ray scattering (SAXS) data were measured on SSRL beamline 4–2 in the range 0.00965 $Å^{-1} \leq q \leq 0.542$ $Å^{-1}$ ($q = 4\pi\sin(\theta)/\lambda$) from solutions of $TLE1_{20–156}$ tetramer at 2.5, 5, 10 and 20 mg/ml. Samples were loaded into a 1.5 mm quartz capillary flow cell maintained at 20°C, and 15 × 1 s exposures were measured for each concentration. The raw scattering data were normalized to the incident beam intensity and buffer scattering subtracted. Individual scattering curves were visually inspected prior to averaging to ensure that radiation damage was minimal. Scattering curves from different concentrations were scaled and merged with PRIMUS (Konarev *et al*, 2003). Scattering amplitudes were calculated from the models with CRYSOL (Svergun *et al*, 1995).

Fluorescent labeling of $TLE1_{20-156}$

Purified $TLE1_{20–156}$ in 25 mM HEPES pH 7.5, 150 mM NaCl, 1 mM EDTA, 2% Glycerol, 5 mM TCEP (Tris (2-carboxyethyl) phosphine) (HEN-buffer) was incubated with 2-fold molar excess of Alexa Fluor 488 C5-Maleimide for 16 h at 4°C on a rotary shaker. A 25-ml Sephadex G-25 column was used to remove the free dye. The eluate was further purified on an analytical S200 column; the labeling efficiency of $TLE1_{20–156}$ was determined to be approximately 95% based on extinction coefficients of the protein and the dye, and the presence of 8 cysteines in the protein.

Fluorescence anisotropy binding assay

Fluorescence anisotropy was carried out with a Synergy 4 Hybrid plate reader using a Corning 3915 black walled 96-well plate. Labeled TLE1-tetramer or dimer at 300 nM was used per well; TCF3, TCF4, LEF1, β-catenin-TCF3 complex or BSA was added at different concentrations into each well. The samples were excited at 485 nm and the emission was measured at 515 nm. All experiments were carried out in HEN-buffer with 0.4% BSA. 40–60 readings were measured per well and were averaged. The averaged anisotropy values were plotted against concentration. The binding isotherm was fit using Eq (1) where Y is fraction bound, $[L]_t$ is the total ligand concentration, R_{max} is the maximum change in anisotropy, K_D is the dissociation constant

$$Y = R_{max}\frac{[L]_t}{([L]_t + K_D)} \quad (1)$$

All experiments were done in duplicate, and the experiments were repeated three independent times. The figures show averaged data points ± standard deviation from the triplicates. The reported K_D values assume that there is no effect of the fluorescent label on the binding affinty; the unstructured nature of TCFs precluded measuring changes in anisotropy if the label was instead on the TCF.

Wnt reporter assay

HEK293 cells were seeded at 2.5×10^5 per 6-well 24 h prior to transfection. Each well was transfected with 0.2 μg Super8xTopflash reporter (kind gift from Dr. RT Moon) and 0.1 μg thymidine kinase β-galactosidase plasmid using BioT transfection reagent (Bioland Scientific). Additional expression vectors were added as needed: 0.4 μg β-catenin, 0.2 μg LEF-1, 0.2 μg TCF-1, 0.2 μg TCF-3, or 0.2 μg TCF-4. The TCF/LEFs were expressed with 2 HA tags at the N-terminus, using the EVR2 vector. Cells were harvested 24 h post transfection and assayed for luciferase activity and β-galactosidase activity (for normalization). Western blots shown in Fig 2B used anti-HA (Genetex #GTX628489, 1:1,000 dilution) for TCF/LEFs and anti-lamin A/C (Cell Signaling #2032, 1:1,000 dilution) for loading controls.

TLE1 tetramer and dimer reporter assay

Activities of the TLE1 dimer and wild-type TLE1 were tested using a Wnt-responsive TOPFlash luciferase reporter assay by transient expression in HEK293T cells. HEK293T cells were seeded in 96-well plates in DMEM containing 10% (v/v) FBS. After 6 h, cells were transiently co-transfected with the SuperTOPFlash Wnt reporter (80 ng) and LacZ expression plasmids (20 ng) for a control, and β-catenin (25 ng), hTCF3 (25 ng) and the indicated TLE1 constructs, using Lipofectamine 2000 according to the manufacturer's protocol. For the cells transfected with TLE1, the media were replaced with mouse L-cell control media (L-cell secreted media without Wnt3a) or purified Wnt3a at 18 h post-transfection. After another 18 h, Luciferase reporter activity was measured in a Veritas Luminometer. Assays were carried out in triplicate, and relative luciferase units were normalized to LacZ.

Hi-Fi FRET assay

Tri-nucleosomes were prepared and quality checked as described in (Winkler *et al*, 2011). Affinity measurements and chromatin labeling were performed as described in (Hieb *et al*, 2012). Alexa-488-labeled TLE tetramer or dimer serve as fluorescent donors, and tri-nucleosomes labeled with Atto-647N dye at a T112C mutation on H2B was the FRET acceptor. Tri-nucleosomes were titrated 0–5 μM concentrations, and $TLE_{20–156}$ tetramer or dimer were kept constant at 1 μM. The experiment was done in 25 mM Tris pH 7.5, 200 mM NaCl, 0.01% NP-40 and CHAPS. FRET data analysis was done as described in (Hieb *et al*, 2012).

Native gel-shift titration binding assays

$TLE_{20–156}$ dimer or tetramer at 10 μM were incubated with increasing concentration of synthetic biotinylated histone tail peptides (Anaspec Inc, Fremont, CA, USA) for 16 h at 4°C. Samples were then run on a 4–20% native PAGE. Proteins were transferred to nitrocellulose membranes and analyzed by Western blotting with Neutravidn-800 for the biotynalted tail, and α-6X-His-680 antibody for TLE1 (loading control). The image was quantified using ImageJ and the data were plotted using the software Prism. The data were fit using Eq (2) where Y is fraction bound, B_{max} is the maximum binding of the ligand, X is the concentration of the Ligand.

$$Y = B_{max} * \frac{X}{(K_d + X)} \quad (2)$$

Supplementary information for this article is available online: http://emboj.embopress.org

Acknowledgements

We thank Matthew L-H. Chu for purified Wnt3A protein and Thomas Weiss for SAXS beamline support. This work was supported by an American Heart Association fellowship to J.V.C., and U.S. National Institutes of Health grants GM56169 to W.I.W. and NIH CA096878, CA108697, P30CA062203 to M.L.W., and P01-GM088409 to K.L. K.L. is also supported by the Howard Hughes Medical Institute. Beamlines at SSRL are supported by the U.S. Department of Energy and the U.S. National Institutes of Health.

Author contributions

JVC purified, crystallized, solved the TLE1-Q structure. JVC designed and performed the protein purification, fluorescence anisotropy binding experiments, TopFlash assays for TLE dimer and tetramer. KTP performed the TopFlash studies of TCF/LEFs. BPT performed the immunofluorescence experiments. MH, UM did the chromatin binding studies. JVC, MLW and WIW wrote the paper with contributions from KL.

Conflict of interest

The authors declare that they have no conflict of interest.

Note added in proof

Fuchs and colleagues (*Nat Cell Biol* 16:179-190 (2014)) have reported specific repressive roles for TCF3/4 in the control of hair follicle stem cell development controlled by Wnt proteins.

References

Adams PD, Afonine PV, Bunkoczi G, Chen VB, Davis IW, Echols N, Headd JJ, Hung LW, Kapral GJ, Grosse-Kunstleve RW, McCoy AJ, Moriarty NW, Oeffner R, Read RJ, Richardson DC, Richardson JS, Terwilliger TC, Zwart PH (2010) PHENIX: a comprehensive Python-based system for macromolecular structure solution. *Acta Crystallogr D Biol Crystallogr* 66: 213 – 221

Arce L, Pate KT, Waterman ML (2009) Groucho binds two conserved regions of LEF-1 for HDAC-dependent repression. *BMC Cancer* 9: 159

Baker NA, Sept D, Joseph S, Holst MJ, McCammon JA (2001) Electrostatics of nanosystems: application to microtubules and the ribosome. *Proc Natl Acad Sci USA* 98: 10037 – 10041

Barbera AJ, Chodaparambil JV, Kelley-Clarke B, Joukov V, Walter JC, Luger K, Kaye KM (2006) The nucleosomal surface as a docking station for Kaposis sarcoma herpesvirus LANA. *Science* 311: 856 – 861

Beagle B, Johnson GV (2010) AES/GRG5: more than just a dominant-negative TLE/GRG family member. *Dev Dyn* 239: 2795 – 2805

Berger SL (2007) The complex language of chromatin regulation during transcription. *Nature* 447: 407 – 412

Billin AN, Thirlwell H, Ayer DE (2000) β-Catenin-histone deacetylase interactions regulate the transition of LEF1 from a transcriptional repressor to an activator. *Mol Cell Biol* 20: 6882 – 6890

Brantjes H, Roose J, van de Wetering M, Clevers H (2001) All Tcf HMG box transcription factors interact with Groucho-related co-repressors. *Nucleic Acids Res* 29: 1410 – 1419

Buscarlet M, Stifani S (2007) The Marx of Groucho on development and disease. *Trends Cell Biol* 17: 353 – 361

Cadigan KM, Waterman ML (2012) TCF/LEFs and Wnt signaling in the nucleus. *Cold Spring Harb Perspect Biol*, 4: a007906.

Chen G, Fernandez J, Mische S, Courey AJ (1999) A functional interaction between the histone deacetylase Rpd3 and the corepressor groucho in *Drosophila* development. *Genes Dev* 13: 2218 – 2230

Chen G, Nguyen PH, Courey AJ (1998) A role for Groucho tetramerization in transcriptional repression. *Mol Cell Biol* 18: 7259 – 7268

Chen VB, Arendall WB, Headd JJ, Keed DA, Immormino RM, Kapral GJ, Murray LW, Richardson JS, Richardson DC (2010) MolProbity: all-atom structure validation for macromolecular crystallography. *Acta Crystallogr* D66: 12 – 21

Chodaparambil JV, Barbera AJ, Lu X, Kaye KM, Hansen JC, Luger K (2007) A charged and contoured surface on the nucleosome regulates chromatin compaction. *Nat Struct Mol Biol* 14: 1105 – 1107

Choi CY, Kim YH, Kim YO, Park SJ, Kim EA, Riemenschneider W, Gajewski K, Schulz RA, Kim Y (2005) Phosphorylation by the DHIPK2 protein kinase modulates the corepressor activity of Groucho. *J Biol Chem* 280: 21427 – 21436

Cowtan K (2006) The Buccaneer software for automated model building. 1. Tracing protein chains. *Acta Crystallogr D Biol Crystallogr* 62: 1002 – 1011

Daniels DL, Weis WI (2005) β-catenin directly displaces Groucho/TLE repressors from Tcf/Lef in Wnt-mediated transcription activation. *Nat Struct Mol Biol* 12: 364 – 371

Dorigo B, Schalch T, Bystricky K, Richmond TJ (2003) Chromatin fiber folding: requirement for the histone H4 N-terminal tail. *J Mol Biol* 327: 85 – 96

Fasolini M, Wu X, Flocco M, Trosset JY, Oppermann U, Knapp S (2003) Hot spots in Tcf4 for the interaction with β-catenin. *J Biol Chem* 278: 21092 – 21098

Fiedler M, Sanchez-Barrena MJ, Nekrasov M, Mieszczanek J, Rybin V, Muller J, Evans P, Bienz M (2008) Decoding of methylated histone H3 tail by the Pygo-BCL9 Wnt signaling complex. *Mol Cell* 30: 507 – 518

Fisher AL, Ohsako S, Caudy M (1996) The WRPW motif of the hairy-related basic helix-loop-helix repressor proteins acts as a 4-amino-acid transcription repression and protein-protein interaction domain. *Mol Cell Biol* 16: 2670 – 2677

Flores-Saaib RD, Courey AJ (2000) Analysis of Groucho-histone interactions suggests mechanistic similarities between Groucho- and Tup1-mediated repression. *Nucleic Acids Res* 28: 4189 – 4196

Gu B, Sun P, Yuan Y, Moraes RC, Li A, Teng A, Agrawal A, Rheaume C, Bilanchone V, Veltmaat JM, Takemaru K, Millar S, Lee EY, Lewis MT, Li B, Dai X (2009) Pygo2 expands mammary progenitor cells by facilitating histone H3 K4 methylation. *J Cell Biol* 185: 811 – 826

Hanson AJ, Wallace HA, Freeman TJ, Beauchamp RD, Lee LA, Lee E (2012) XIAP monoubiquitylates Groucho/TLE to promote canonical Wnt signaling. *Mol Cell* 45: 619 – 628

Hasson P, Egoz N, Winkler C, Volohonsky G, Jia S, Dinur T, Volk T, Courey AJ, Paroush Z (2005) EGFR signaling attenuates Groucho-dependent repression to antagonize Notch transcriptional output. *Nat Genet* 37: 101 – 105

Hasson P, Paroush Z (2007) Crosstalk between the EGFR and other signalling pathways at the level of the global transcriptional corepressor Groucho/TLE. *Br J Cancer* 96(Suppl): R21 – R25

Hecht A, Vleminckx K, Stemmler MP, van Roy F, Kemler R (2000) The p300/CBP acetyltransferases function as transcriptional coactivators of β-catenin in vertebrates. *EMBO J* 19: 1839 – 1850

Hieb AR, D'Arcy S, Kramer MA, White AE, Luger K (2012) Fluorescence strategies for high-throughput quantification of protein interactions. *Nucleic Acids Res* 40: e33

Hikasa H, Ezan J, Itoh K, Li X, Klymkowsky MW, Sokol SY (2010) Regulation of TCF3 by Wnt-dependent phosphorylation during vertebrate axis specification. *Dev Cell* 19: 521 – 532

Hikasa H, Sokol SY (2011) Phosphorylation of TCF proteins by homeodomain-interacting protein kinase 2. *J Biol Chem* 286: 12093 – 12100

Jessen S, Gu B, Dai X (2008) Pygopus and the Wnt signaling pathway: a diverse set of connections. *BioEssays* 30: 448 – 456

Jimenez G, Paroush Z, Ish-Horowicz D (1997) Groucho acts as a corepressor for a subset of negative regulators, including Hairy and Engrailed. *Genes Dev* 11: 3072 – 3082

Kabsch W (2010) Integration, scaling, space-group assignment and post-refinement. *Acta Crystallogr D Biol Crystallogr* 66: 133 – 144

Kim CH, Oda T, Itoh M, Jiang D, Artinger KB, Chandrasekharappa SC, Driever W, Chitnis AB (2000) Repressor activity of Headless/Tcf3 is essential for vertebrate head formation. *Nature* 407: 913 – 916

Knapp S, Zamai M, Volpi D, Nardese V, Avanzi N, Breton J, Plyte S, Flocco M, Marconi M, Isacchi A, Caiolfa VR (2001) Thermodynamics of the high-affinity interaction of TCF4 with β-catenin. *J Mol Biol* 306: 1179 – 1189

Konarev PV, Volkov VV, Sokolova AV, Koch MHJ, Svergun DI (2003) PRIMUS: a windows PC-based system for small-angel scattering data analysis. *J Appl Crystallogr* 36: 1277 – 1282

Korinek V, Barker N, Willert K, Molenaar M, Roose J, Wagenaar G, Markman M, Lamers W, Destree O, Clevers H (1998) Two members of the Tcf family implicated in Wnt/beta-catenin signaling during embryogenesis in the mouse. *Mol Cell Biol* 18: 1248 – 1256

Kuo D, Nie M, De Hoff P, Chambers M, Phillips M, Hirsch AM, Courey AJ (2011) A SUMO-Groucho Q domain fusion protein: characterization and in vivo Ulp1-mediated cleavage. *Protein Expr Purif* 76: 65 – 71

Laskowski RA, MacArthur MW, Moss DS, Thornton JM (1993) PROCHECK: a program to check the stereochemical quality of protein structures. *J Appl Crystallogr* 26: 283 – 291

Lee W, Swarup S, Chen J, Ishitani T, Verheyen EM (2009) Homeodomain-interacting protein kinases (Hipks) promote Wnt/Wg signaling through stabilization of beta-catenin/Arm and stimulation of target gene expression. *Development* 136: 241 – 251

Liu F, van den Broek O, Destree O, Hoppler S (2005) Distinct roles for Xenopus Tcf/Lef genes in mediating specific responses to Wnt/β-catenin signalling in mesoderm development. *Development* 132: 5375 – 5385

Logan CY, Nusse R (2004) The Wnt signaling pathway in development and disease. *Annu Rev Cell Dev Biol* 20: 781 – 810

Merrill BJ, Pasolli HA, Polak L, Rendl M, Garcia-Garcia MJ, Anderson KV, Fuchs E (2004) Tcf3: a transcriptional regulator of axis induction in the early embryo. *Development* 131: 263 – 274

Nguyen H, Merrill BJ, Polak L, Nikolova M, Rendl M, Shaver TM, Pasolli HA, Fuchs E (2009) Tcf3 and Tcf4 are essential for long-term homeostasis of skin epithelia. *Nat Genet* 41: 1068 – 1075

Nuthall HN, Joachim K, Palaparti A, Stifani S (2002) A role for cell cycle-regulated phosphorylation in Groucho-mediated transcriptional repression. *J Biol Chem* 277: 51049 – 51057

Palaparti A, Baratz A, Stifani S (1997) The Groucho/transducin-like enhancer of split transcriptional repressors interact with the genetically defined amino-terminal silencing domain of histone H3. *J Biol Chem* 272: 26604 – 26610

Patel SR, Bhumbra SS, Paknikar RS, Dressler GR (2012) Epigenetic mechanisms of Groucho/Grg/TLE mediated transcriptional repression. *Mol Cell* 45: 185 – 195

Pereira L, Yi F, Merrill BJ (2006) Repression of Nanog Gene Transcription by Tcf3 Limits Embryonic Stem Cell Self-Renewal. *Mol Cell Biol*, 26: 7479 – 7491

Polakis P (2007) The many ways of Wnt in cancer. *Curr Opin Genet Dev* 17: 45 – 51

Roose J, Huls G, van Beest M, Moerer P, van der Horn K, Goldschmeding R, Logtenberg T, Clevers H (1999) Synergy between tumor suppressor APC and the beta-catenin-Tcf4 target Tcf1. *Science* 285: 1923 – 1926

Schiltz M, Bricogne G (2007) Modelling and refining site-specific radiation damage in SAD/MAD phasing. *J Synchrotron Radiat* 14: 34 – 42

Sekiya T, Zaret KS (2007) Repression by Groucho/TLE/Grg proteins: genomic site recruitment generates compacted chromatin in vitro and impairs activator binding in vivo. *Mol Cell* 28: 291 – 303

Semenyuk AV, Svergun DI (1991) GNOM - a program package for small-angle scattering data processing. *J Appl Crystallogr* 24: 537 – 540

Sierra J, Yoshida T, Joazeiro CA, Jones KA (2006) The APC tumor suppressor counteracts β-catenin activation and H3K4 methylation at Wnt target genes. *Genes Dev* 20: 586 – 600

Song H, Hasson P, Paroush Z, Courey AJ (2004) Groucho oligomerization is required for repression in vivo. *Mol Cell Biol* 24: 4341 – 4350

Standley HJ, Destree O, Kofron M, Wylie C, Heasman J (2006) Maternal XTcf1 and XTcf4 have distinct roles in regulating Wnt target genes. *Dev Biol* 289: 318 – 328

Suganuma T, Workman JL (2011) Signals and combinatorial functions of histone modifications. *Annu Rev Biochem* 80: 473 – 499

Sun J, Weis WI (2011) Biochemical and structural characterization of beta-catenin interactions with nonphosphorylated and CK2-phosphorylated Lef-1. *J Mol Biol* 405: 519 – 530

Svergun D, Barberato C, Koch MHJ (1995) CRYSOL: a program to evaluate x-ray solution scattering of biological macromolecules from atomic coordinates. *J Appl Crystallogr* 28: 768 – 773

Takemaru K, Moon RT (2000) The transcriptional coactivator CBP interacts with β-catenin to activate gene expression. *J Cell Biol* 149: 249 – 254

Tam WL, Lim CY, Han J, Zhang J, Ang YS, Ng HH, Yang H, Lim B (2008) T-cell factor 3 regulates embryonic stem cell pluripotency and self-renewal by the transcriptional control of multiple lineage pathways. *Stem Cells* 26: 2019 – 2031

Tang W, Dodge M, Gundapaneni D, Michnoff C, Roth M, Lum L (2008) A genome-wide RNAi screen for Wnt/beta-catenin pathway components identifies unexpected roles for TCF transcription factors in cancer. *Proc Natl Acad Sci USA* 105: 9697 – 9702

Turki-Judeh W, Courey AJ (2012) Groucho: a corepressor with instructive roles in development. *Curr Top Dev Biol* 98: 65 – 96

van de Wetering M, Cavallo R, Booijes D, van Beest M, van Es J, Loureiro J, Ypma A, Hursh D, Jones T, Bejsovec A, Peifer M, Mortin M, Clevers H (1997) Armadillo coactivates transcription driven by the product of the *Drosophila* segment polarity gene *dTCF*. *Cell* 88: 789 – 799

Winkler DD, Muthurajan UM, Hieb AR, Luger K (2011) Histone chaperone FACT coordinates nucleosome interaction through multiple synergistic binding events. *J Biol Chem* 286: 41883 – 41892

Winn MD, Ballard CC, Cowtan KD, Dodson EJ, Emsley P, Evans PR, Keegan RM, Krissinel EB, Leslie AG, McCoy A, McNicholas SJ, Murshudov GN, Pannu NS, Potterton EA, Powell HR, Read RJ, Vagin A, Wilson KS (2011) Overview of the CCP4 suite and current developments. *Acta Crystallogr D Biol Crystallogr* 67: 235 – 242

Wu B, Piloto S, Zeng W, Hoverter NP, Schilling TF, Waterman ML (2013) Ring Finger Protein 14 is a new regulator of TCF/beta-catenin-mediated transcription and colon cancer cell survival. *EMBO Rep* 14: 347 – 355

Yi F, Pereira L, Hoffman JA, Shy BR, Yuen CM, Liu DR, Merrill BJ (2011) Opposing effects of Tcf3 and Tcf1 control Wnt stimulation of embryonic stem cell self-renewal. *Nat Cell Biol* 13: 762 – 770

Zhou J, Fan JY, Rangasamy D, Tremethick DJ (2007) The nucleosome surface regulates chromatin compaction and couples it with transcriptional repression. *Nat Struct Mol Biol* 14: 1070 – 1076